BIONANOSCAFFOLDS-ENABLED NON-WETTING SURFACES FOR ANTIBIOFOULING APPLICATIONS

Sangwook Chu[1,2], Ishita Shahi[1], Ryan C. Huiszoon[1,2,4], James N. Culver[4,5], and Reza Ghodssi[1,2,3,4]*
[1]MEMS Sensors and Actuators Lab, [2]Institute for Systems Research,
[3]Department of Electrical and Computer Engineering, [4]Fischell Department of Bioengineering,
[5]Institute for Bioscience and Biotechnology Research,
Department of Plant Science and Landscape Architecture,
University of Maryland, College Park, MD, USA

ABSTRACT

This paper presents biological nano-scaffolds (BNS)-assisted formation of non-wetting polymeric surfaces with excellent antibiofouling performance. Particularly, Tobacco mosaic virus (TMV)-templated metallic nanoscaffolds, self-assembled on Au substrates followed by a simple spin-and-dry coating of a fluorinated polymer solution, provide complex micro/nanoscale structured surfaces with non-wetting properties. The BNS-based superhydrophobic surfaces demonstrated significantly enhanced water-repellent properties compared to a planar/non-structured counterpart, 1) showing no sign of solid-liquid attraction (contact angle: ~180º) with DI water, and 2) achieving complete and repeated droplet bouncing without surface pinning events. More significantly, in a static 48-hour biofilm growth experiment, the BNS-based superhydrophobic surfaces resulted in a 6-fold reduction in adherent biofilm compared to their planar counterparts, most likely attributed to the extreme non-adherent property combined with complex surface morphology. Combined results provide a simple and powerful method for achieving the robust non-wetting/anti-biofouling surfaces needed in a broad range of applications.

KEYWORDS

Biological scaffolds, Biofouling, Biofilm, Non-wetting, Superhydrophobic surfaces.

INTRODUCTION

Prevention of bacterial biofilm formation on surfaces has been a pertinent challenge in a wide range of human health-associated domains [1]. In particular, biofilms, are the primary cause of nosocomial infections - responsible for 62% of all hospital-acquired infections in the US - many hospitalized patients are exposed to surgical procedures or clinical practices that increase the likelihood of vulnerable body sectors (e.g. implant sites, blood vessels, urinary tract) being accessed by pathogenic bacteria [2], [3]. Another impending concern are biofilms in public/industrial water systems, particularly on water pipelines and filter/purification membranes, which poses a significant threat to all human water resources [4].

There have been numerous strategies developed over the past decades involving physicochemical mechanisms to address these biofilm-associated challenges. Some of the major approaches include the development of bacterial-communication molecule analogs (e.g. AI-2) [5], surface functionalization of antimicrobial peptides [6], fabrication of bioinspired hydrophobic/3-D structured surfaces [7], [8], and incorporation of the bioelectric effect that combines an electric-field with small dosage of antibiotics [9]. These approaches have primarily focused on demonstrating retardation, removal, or prevention of biofilm growth - in conjunction with zero or reduced dosages of antibiotics - on a wide range of vulnerable surfaces.

As biofilm formation on surfaces is driven by bacterial adherence followed by inter-molecular communication, a promising strategy for mitigating surface fouling events has been the development of non-adherent, superhydrophobic surface coatings displaying micro/nanoscale surface structures that could potentially help disrupt bacterial adherence or communication [10]. In our recent work, we have developed a 3-D electro-bioprinting (3-D EBP) technique that allows assembly of hierarchical surface topology with high scalability by combining the bottom-up assembly of biological nanoscaffolds (BNS), cysteine-modified Tobacco mosaic virus (TMV1cys), with top-down fabricated microstructures [11]. In an effort to leverage this manufacturing capability for studying the potential relationships between hydrophobic 3-D micro-/nano-scale surface topologies and biofilm growth, this work has focused on developing hydrophobic coating strategies over TMV-templated nanostructures and characterizing their performance in mitigating biofilm growth.

MATERIALS AND METHODS

BNS-assisted Superhydrophobic Surfaces

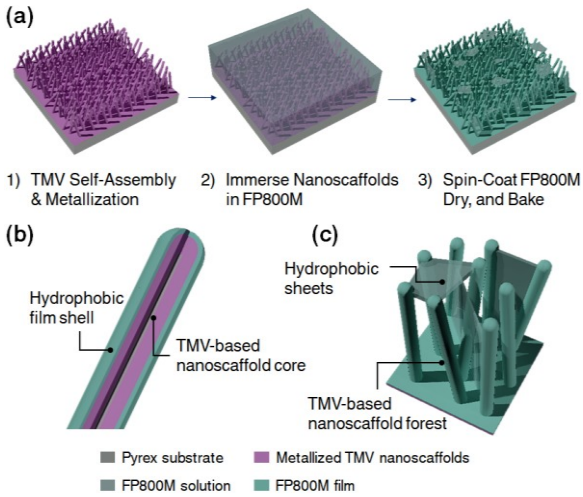

Figure 1: Schematics of (a) process flow for creating BNS-based superhydrophobic surfaces and (b-c) major mechanisms involved in the formation of the complex hydrophobic structure.

TMV, the BNS in this work, is a plant virus displaying a nanoscale high-aspect-ratio structure (diameter: 18nm, length: 300nm) that has been utilized as a versatile template for the development of a wide range of nanotechnology-driven applications [12]. Over the past decade, our group and collaborators have extensively utilized TMV1cys for the development of miniaturized energy storage devices (e.g. micro -batteries and -supercapacitors) [13], [14], which have leveraged the high affinity of thiol to metals, that ultimately provides both the surface immobilization and conformal metallization mechanisms essential for creating robust nanostructured surfaces.

As illustrated in Figure 1a, the BNS surfaces are comprised of electroless-metallized TMV1cys which were first prepared on Ti (10nm)/Au (200nm) deposited glass substrates (5×5mm^2) via self-assembly of TMV1cys followed by Ni electroless metallization [13]. Introduction of 5µL of hydrophobic polymer solution (FluoroPel 800M (FP800M), Cytonix) allowed complete immersion of the BNS. This was followed by a spin coating step (2000 rpm for 30 seconds) which facilitated spreading and instant drying of the FP800M solution. After curing at 160°C on a hotplate for 5 minutes, the superhydrophobic surfaces displayed complex micro- and nano-scale structures as depicted in Figure 1a. As shown in Figure 1b and 1c, respectively, two major film-forming mechanisms have been considered in this approach: 1) Conformal 3-D coating over the BNS creating core-shell structures (Figure 1b), and 2) formation of 2-D micro and nanoscale sheets between the neighboring scaffolds leveraging surface tension (Figure 1c).

Characterization of Surface Wettability

The surface morphology of the BNS-templated FP800M (BNS-FP800M) surface has been characterized using SEM (Hitachi S-3400) in comparison with surfaces coated only with either TMV1cys or FP800M. Surface wettability of the BNS-FP800M has been evaluated by monitoring liquid pinning events of DI water on the surfaces, as well as by capturing droplet bouncing events using a high speed camera (Redlake MotionPro HS-3, images captured at 1kHz), both in comparison with planar-FP-800M.

Characterization of Biofilm Growth

As described in Figure 2a, biofilm growth experiments were performed in a static environment using *Escherichia coli* (*E. coli*) K12 W3110 bacteria that had been cultured overnight and diluted to an OD_{600} of 0.25. Three different surfaces - Planar Au, Planar-FP800M, BNS-FP800M - have been co-incubated in a parafilm-coated plastic petri-dish during a 48-hour biofilm growth period at 37° in Lysogeny broth (LB) media. Planar Au has been included as a hydrophilic control to investigate the effect of surface hydrophobicity without the BNS-based surface topology (Planar-FP800M). Planar-FP800M has been prepared using identical process steps described above, excluding the TMV1cys self-assembly. It should be noted that the volume of LB media was adjusted to ensure complete immersion of the BNS-FP800M surfaces is achieved throughout the biofilm growth period. Additionally, LB media was replenished after 24-hours to prevent depletion of nutrients. After the 48-hour growth period, all three samples were collected from the petri-dish and stained with syto9 for evaluation of the biofilm growth under a fluorescence microscope (Leica INM100).

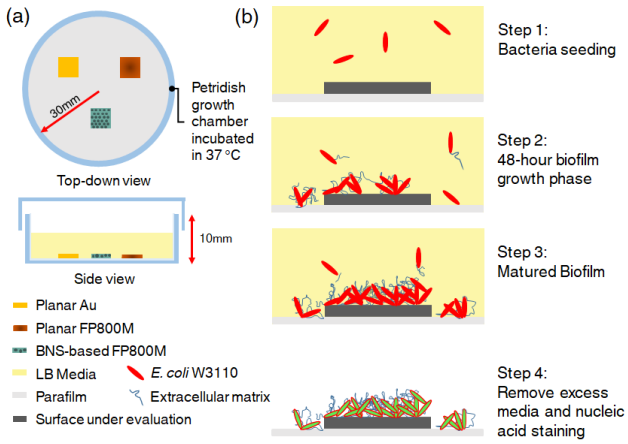

Figure 2: Schematics of the biofilm formation experiment. (a) Three different surfaces (planar Au, planar FP800M, and BNS-based FP800M) were co-incubated at 37°C. (b) Bacteria culture (E. coli K12 W3110, OD: 0.25) was seeded for 2 hours, followed by a 48-hour growth phase with LB media replenished after 24 hours. Matured biofilm was syto9-stained for evaluation of biofilm on the surfaces.

RESULTS AND DISCUSSIONS

Surface Morphology and Wettability

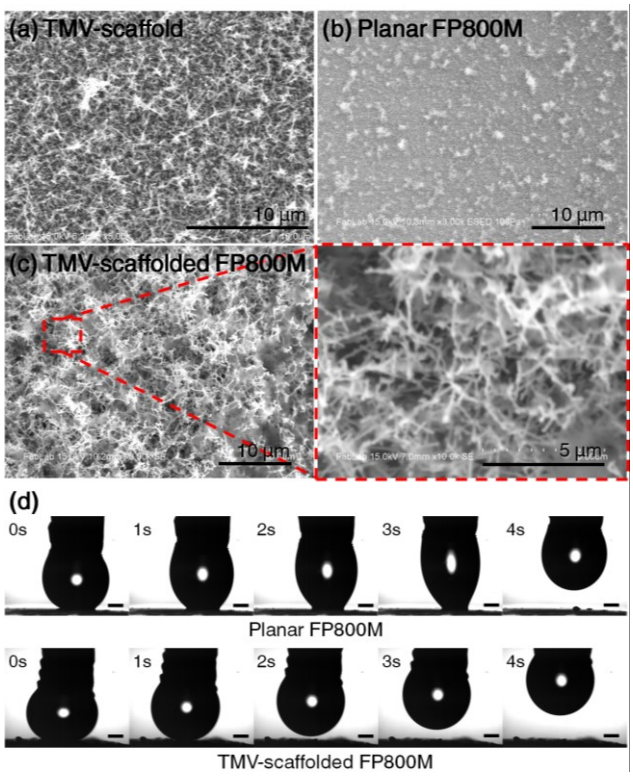

Figure 3. Comparisons of (a-c) surface morphologies between TMV1cys-only, FP800M-only, and BNS-FP800M surfaces, and (d) observations of DI water droplet being withdrawn from planar- and BNS- FP800M (scale bar: 0.5 mm unless specified).

The SEM images shown in Figure 3a-c, compare the surface morphology of three surface types -

TMV1cys-only, FP800M-only, and BNS-FP800M - confirming the formation of a complex hydrophobic surface topology with BNS. As discussed earlier, the spin-dry coating of FP800M on the BNS induced the formation of a conformal coating over individual BNS as well as the 2-D micro/nanosheets in between the scaffolds (gray regions between BNS in Figure 3c), ultimately contributing to an overall increase in surface morphology heterogeneity (Figure 3c), leading to enhanced hydrophobicity. A comparison of optical images shown in Figure 3d, where 7 µL-droplets of DI water are being slowly separated from the two different surfaces (planar- and BNS- FP800M), confirms the successful formation of the BNS-based superhydrophobic surfaces as seen by the corresponding enhancement in water repellent property, showing no measurable solid-liquid attraction (e.g. pinning) compared to that observed from planar-FP800M surfaces. The enhanced water repelling property of the BNS-FP800M surfaces has been further characterized by monitoring droplet bouncing events as shown in Figure 4. The 7 µL DI water droplet was suspended and released from a ~30 mm height (determined as the maximum height where no droplet fragmentation would occur upon impact with the surface) onto the planar-FP800M surface (Figure 4a) resulted in only a single bounce, with the droplet settling on the surface during the second impact, as compared to the three bounces achieved with BNS-FP800M surfaces (Figure 4b, each row shows frame sequences for each bouncing event starting at time zero) at a relatively high velocity of 2 m/s at the point of impact. Consequently, during the fourth surface impact the droplet fell off the sample region, and additional bouncing events could not be observed without improvement to the experimental stage to achieve a horizontally flat plane. Based on a report by Crick et al. [15], there is a strong correlation between the number of droplet bouncing events versus the surface hydrophobicity, this theory strongly supports the observed enhancement to the water repelling property of the BNS-FP800M demonstrating a near non-wetting characteristic. Due to the severe water repelling property of the BNS-FP800M, droplet contact angle could not be measured.

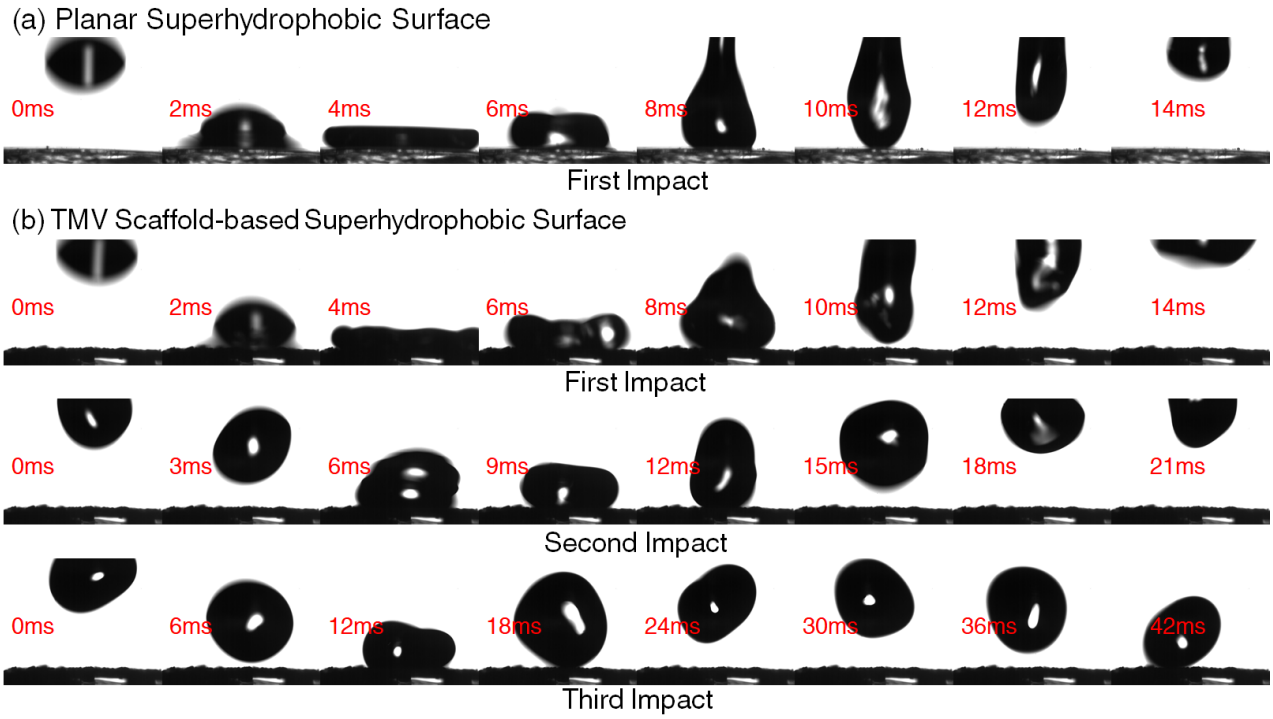

Figure 4. Arrays of frame sequences (taken with highspeed camera at 1kHz) comparing a droplet of DI water (7µL falling at ~ 2m/s for the first surface impact) bouncing on (a) planar and (b) BNS-based superhydrophobic surfaces. Frame sequences per consecutive bouncing events are taken at different time intervals (1st: 2ms, 2nd: 3ms, 3rd: 6ms) due to the decrease in kinetic energy of the droplet after each bouncing.

Significant Reduction in Biofilm Growth

Figure 5 shows the fluorescence microscopy analysis of the biofilm growth on different surfaces. After the 48-hour growth period, the primary observation indicated that all three surfaces were covered with the slimy extracellular matrix representative of the biofilm. This indicates that the superhydrophobic characteristics of both the planar- and BNS- FP800M surfaces have been lost while being immersed in the growth media. However, when comparing the fluorescence intensities of the syto-9 stained surfaces, as shown in Figure 5, the super-repellant BNS-FP800M surfaces demonstrated an excellent anti-biofouling performance at the conclusion of the 48-hour growth period compared to the other controls, resulting in ~75% and ~83% reduction in biofilm formation compared to planar -hydrophilic (planar Au) and -hydrophobic (FP800M) surfaces, respectively. Considering that the surface energy of the planar-FP800M was also in the superhydrophobic regime (based on a contact angle > 150° from vendor specifications and the droplet bouncing event analysis), the results indicate that the complex surface topology at the micro/nanoscale have played a critical role in mitigating the biofilm formation. However, considering that the slimy substances were

observed on all surfaces after the growth period, the authors believe that the BNS-FP800M surfaces would have eventually been colonized by biofilms if the growth experiments had been prolonged, to similar levels observed from the other two surfaces, requiring further investigations.

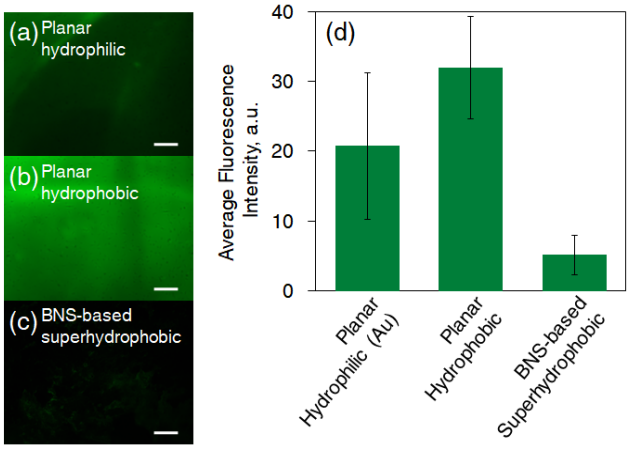

Figure 5: Fluorescence microscopy analysis of bacterial biofilm formation on different surfaces after a 48-hour growth-period. Both the planar -hydrophilic (a, bare Au) and -hydrophobic (b, FP800M) surfaces displayed a significantly higher amount of biofilm compared to the (c) BNS-based superhydrophobic surfaces. (n=3 for error bars of each surface type in plot (d), scale bar: 100μm).

CONCLUSIONS

In this work, a simple strategy for creating heterogeneously structured antibiofouling surfaces has been demonstrated leveraging TMV-based BNS to help mitigate bacterial biofilm formation. The excellent water repelling/non-wetting property combined with the result of significantly mitigated biofilm growth under static environmental conditions strongly supports BNS-FP800M as a potential solution for creating robust antibiofouling surfaces. This is the initial stage towards development of BNS-assisted non-adherent surfaces which have focused on investigating the impact of sub-micron scale surface topology on biofilm growth. Future efforts will incorporate surface topologies across a broader range of scales with longer term growth experiments.

ACKNOWLEDGEMENTS

This work was funded by the Biochemistry Program of the Army Research Office (W911NF-17-1-0137) and National Science Foundation (ECCS-1809436). The authors acknowledge the support of the Maryland Nanocenter and its FabLab for support during fabrication and imaging processes.

REFERENCES

[1] H. C. Flemming, J. Wingender, U. Szewzyk, P. Steinberg, S. A. Rice, and S. Kjelleberg, "Biofilms: An emergent form of bacterial life," *Nature Reviews Microbiology.*, vol. 14, no. 9, pp. 563–575, 2016.

[2] M. Habash and G. Reid, "Microbial biofilms: Their development and significance for medical device-related infections," *Journal of Clinical Pharmacology*, vol. 39, no.9, pp.887–898, 1999.

[3] R. Lynfield *et al.*, "Multistate Point-Prevalence Survey of Health Care–Associated Infections," *N. Engl. J. Med.*, vol. 370, pp. 1198–1208, 2014.

[4] C. S. Ong, P. S. Goh, W. J. Lau, N. Misdan, and A. F. Ismail, "Nanomaterials for biofouling and scaling mitigation of thin film composite membrane: A review," *Desalination*, vol. 393, pp. 2–15, 2016.

[5] V. Roy *et al.*, "AI-2 analogs and antibiotics: A synergistic approach to reduce bacterial biofilms," *Appl. Microbiol. Biotechnol.*, vol. 97, no. 6, pp. 2627–2638, 2013.

[6] G. Gao *et al.*, "The biocompatibility and biofilm resistance of implant coatings based on hydrophilic polymer brushes conjugated with antimicrobial peptides," *Biomaterials*, vol. 32, no. 16, pp. 3899–3909, Jun. 2011.

[7] R. Rosenzweig, K. Perinbam, V. K. Ly, S. Ahrar, A. Siryaporn, and A. F. Yee, "Nanopillared Surfaces Disrupt *Pseudomonas aeruginosa* Mechanoresponsive Upstream Motility," *ACS Appl. Mater. Interfaces*, vol. 11, no. 11, pp. 10532–10539, Mar. 2019.

[8] L. E. Fisher, Y. Yang, M.-F. Yuen, W. Zhang, A. H. Nobbs, and B. Su, "Bactericidal activity of biomimetic diamond nanocone surfaces," *Biointerphases*, vol. 11, no. 1, p. 011014, Mar. 2016.

[9] Y. W. Kim *et al.*, "Effect of electrical energy on the efficacy of biofilm treatment using the bioelectric effect," *npj Biofilms Microbiomes*, vol. 1, no. 1, p. 15016, Dec. 2015.

[10] A. J. Scardino, H. Zhang, D. J. Cookson, R. N. Lamb, and R. de Nys, "The role of nano-roughness in antifouling," *Biofouling*, vol. 25, no. 8, pp. 757–767, 2009.

[11] S. Chu, T. E. Winkler, A. D. Brown, J. N. Culver, and R. Ghodssi, "Localized Three-Dimensional Functionalization of Bionanoreceptors on High-Density Micropillar Arrays via Electrowetting," *Langmuir*, vol 34, no. 4, pp. 1725–1732, Jan. 2018.

[12] S. Chu, A. D. Brown, J. N. Culver, and R. Ghodssi, "Tobacco Mosaic Virus as a Versatile Platform for Molecular Assembly and Device Fabrication," *Biotechnol. J.*, vol. 13, no. 12, p.1800147, 2018.

[13] K. Gerasopoulos *et al.*, "Hierarchical three-dimensional microbattery electrodes combining bottom-up self-assembly and top-down micromachining," *ACS Nano*, vol. 6, no. 7, pp. 6422–6432, 2012.

[14] S. Chu, K. Gerasopoulos, and R. Ghodssi, "Tobacco mosaic virus-templated hierarchical Ni/NiO with high electrochemical charge storage performances," *Electrochim. Acta*, vol. 220, pp. 184–192, 2016.

[15] C. R. Crick and I. P. Parkin, "Water droplet bouncing-a definition for superhydrophobic surfaces," *Chem. Commun.*, vol. 47, pp. 12059–12061, 2011.

CONTACT

*R. Ghodssi, tel: +1-301-4058158; ghodssi@umd.edu